JCN Open Access ORIGINAL ARTICLE

pISSN 1738-6586 / eISSN 2005-5013 / J Clin Neurol 2020;16(4):562-572 / https://doi.org/10.3988/jcn.2020.16.4.562

Paramagnetic Rims in Multiple Sclerosis and Neuromyelitis Optica Spectrum Disorder: A Quantitative Susceptibility Mapping Study with 3-T MRI

Jinhee Jang[a]
Yoonho Nam[a,b]
Yangsean Choi[a]
Na-Young Shin[a]
Jae Young An[c]
Kook-Jin Ahn[a]
Bum-soo Kim[a]
Kwang-Soo Lee[d]
Woojun Kim[d]

[a]Departments of Radiology and [d]Neurology, Seoul St. Mary's Hospital, College of Medicine, The Catholic University of Korea, Seoul, Korea
[b]Division of Biomedical Engineering, Hankuk University of Foreign Studies, Yongin, Korea
[c]Department of Neurology, St. Vincent's Hospital, College of Medicine, The Catholic University of Korea, Suwon, Korea

Background and Purpose Iron retained by activated microglia and macrophages in multiple sclerosis (MS) lesions may serve as a marker of innate immune system activation. Among several magnetic resonance imaging (MRI) methods, there has been recent interest in using quantitative susceptibility mapping (QSM) as a potential tool for assessing iron levels in the human brain. This study examined QSM findings in MS and neuromyelitis optica spectrum disorder (NMOSD) lesions obtained with 3-T MRI to assess imaging characteristics related to paramagnetic rims around brain lesions in MS and NMOSD.

Methods This study included 32 MS and 21 seropositive NMOSD patients. MRI images were obtained using two 3-T MRI devices (Ingenia, Philips Healthcare; and Magnetom Verio, Siemens Healthineers) during routine diagnosis and treatment procedures. Multi and single echo gradient echo magnitude and phase images were obtained for QSM reconstruction. QSM images were used to characterize the detected lesions, and the findings were compared between MS and NMOSD.

Results Totals of 71 and 35 MRI scans were performed during the study period in MS and NMOSD patients, respectively. In QSM images, paramagnetic rims were found in 26 (81.2%) MS patients and 1 (4.8%) NMOSD patient. Eight of the 22 MS patients and only 1 of the 10 NMOSD patients who underwent follow-up MRI showed new paramagnetic rims. The paramagnetic rim lesions appeared after enhancement or in new T2-weighted lesions without enhancement.

Conclusions Paramagnetic rims might be a characteristic MRI finding for MS, and therefore they have potential as an imaging marker for differentially diagnosing MS from NMOSD using 3-T MRI.

Key Words multiple sclerosis, neuromyelitis optica spectrum disorder, quantitative susceptibility mapping, iron, demyelination, magnetic resonance imaging.

INTRODUCTION

Multiple sclerosis (MS) is a chronic inflammatory and degenerative disease of the central nervous system that is characterized by multifocal demyelination from an autoimmune response to self-antigens in genetically susceptible individuals.[1] An early differential diagnosis of MS from other possible diseases, including neuromyelitis optica spectrum disorder (NMOSD), is crucial for its optimal management.[2,3] Although the concepts of these two diseases have become more obvious and new diagnostic criteria have been published,[4,5] correct differential diagnoses remain challenging, particularly in NMOSD patients with brain MRI lesions.

Received November 1, 2019
Revised May 15, 2020
Accepted May 15, 2020

Correspondence
Woojun Kim, MD
Department of Neurology, Seoul St. Mary's Hospital, College of Medicine, The Catholic University of Korea, 222 Banpo-daero, Seocho-gu, Seoul 06591, Korea
Tel +82-2-2258-2815
Fax +82-2-599-9686
E-mail wjkim@catholic.ac.kr

Iron plays an important role in neuroinflammatory diseases, including MS, and so iron retained by activated microglia and macrophages in MS lesions may serve as a marker of innate immune system activation. Activated microglia are typically present in the vicinity of chronic active MS lesions and are the predominant source of iron within these lesions. The iron content changes significantly as lesions develop from active demyelination to chronic inflammation and chronic inactivity.[6-10] Abnormally high iron concentrations have been reported in the subcortical gray matter and lesions of MS patients.[11]

Several magnetic resonance imaging (MRI) methods have been introduced for the in vivo imaging of iron in MS lesions. Among them, there has been recent interest in quantitative susceptibility mapping (QSM) as a potential tool for assessing iron levels in the human brain, including MS lesions.[12,13] QSM is a method that estimates the bulk susceptibility of imaging voxels.[14] Compared with conventional T2-weighted images or susceptibility-weighted images (SWI), QSM can offer better visualization and quantification of susceptibility sources in the normal and pathologic tissues of demyelinating lesions.[15-18] Specifically, SWI exploit both magnitude and phase information to highlight tissues with paramagnetic properties, such as hemorrhages. While SWI provides excellent depictions of tiny paramagnetic lesions such as microbleeds, they still rely on nonlocal phase information, and the blooming artifact can mask the details of small lesions. Also, SWI do not accentuate non-linear-shaped paramagnetic structures well. On the other hand, QSM gives detailed information on the local distribution of magnetic susceptibility in the brain. Hence, QSM can demonstrate subtle regional variations of magnetic susceptibility that are not evident in SWI.[19] Moreover, it can provide good contrast for iron deposition in MS lesions thanks to the strong paramagnetic property of iron.[10,18]

A previous study explored the diagnostic value of QSM in MS and NMOSD using 7-T MRI, and suggested that iron-laden lesions in ultra-high-field MRI were characteristic findings in MS compared to NMOSD.[15] Among various forms of iron deposition in MS lesions, studies using 7-T MRI have suggested that iron-related rims are unique to MS lesions.[7,20] Thus, the presence of these rims might be useful for distinguishing MS from other demyelinating diseases. However, 7-T MRI is not widely available, and so its images are not suitable as a reference standard for the differential diagnosis of MS. Few studies have used 3-T MRI to investigate the paramagnetic rims in MS and their clinical characteristics.[21-23] In addition, while the magnetic susceptibility of MS lesions shows dynamic changes[18,20] in line with other MRI findings of MS lesions, there have been only a few reports on the development of iron-laden, paramagnetic rims around MS lesions and their temporal changes.[23,24] Knowledge about these MRI findings relating to MS inflammation might help broaden our understanding of the pathophysiology underlying this complex disease.

In this study we investigated the QSM findings of MS lesions in 3-T MRI. We assessed the prevalence of paramagnetic rims in MS lesions in comparison with NMOSD lesions. We also explored the diagnostic performance of these QSM findings, as well as the temporal changes of paramagnetic rims in both MS and NMOSD patients.

METHODS

Subjects

This retrospective study reviewed the medical records in our hospital and included all MS and NMOSD patients who underwent MRI from January 2015 to December 2018. The study enrolled 32 patients with definite MS as determined by the 2017 McDonald criteria,[4] all of whom were the relapsing-remitting type, and 21 NMOSD patients who showed positivity for serum anti-aquaporin-4 IgG in a cell-based immunohistochemistry test.[5] Patients suffering from other systemic chronic illnesses or injury were excluded from the study.

Patient demographics and clinical characteristics were collected on age, sex, disease duration, Expanded Disability Status Scale (EDSS) score, MRI examination date, treatments received, and disease status when MRI was performed. This study was approved by the Institutional Review Board of the Seoul St. Mary's Hospital, Seoul, Korea (approval no.: KC18RESI0342), which waived the requirement to obtain informed consent due to the noninterventional and retrospective design of the study.

MRI evaluations

MRI scans were performed during routine diagnosis and treatment procedures. MRI was generally performed at the first diagnosis, during routine follow-ups (usually every year), and when relapses were suspected.

MRI images were obtained using one of two 3-T MRI (Ingenia, Philips Healthcare, Best, the Netherlands; and Magnetom Verio, Siemens Healthineers, Erlangen, Germany) with a phased array coil with 32 channels (for the Ingenia) or 12 channels (for the Magnetom Verio) depending on the clinical circumstances. QSM utilized multi-echo [echo time (TE)=7.2, 13.4, 19.6, and 25.8 msec for the Magnetom Verio, or TE=5.8, 12.0, 18.2, 24.4, 30.6, and 36.8 msec for the Ingenia] or single echo (TE=20 msec for the Magnetom Verio device) gradient echo magnitude and phase images obtained for susceptibility-weighted imaging, which is one of the protocols recommended by the MS Consortium.[25] The QSM processing involved the following steps: 1) phase unwrapping for the phase image at each echo time,[26] 2) calculation of the combined frequency for each

voxel from the (multi-echo) phase images,[27] 3) brain masking[28] and removal of the background frequency,[27] and 4) QSM calculation using the iLSQR method.[29] Because cusp artifacts in the phase images or an incorrectly generated brain mask can create severe errors in QSM calculations,[30] an MRI physicist checked for such errors before the region-of-interest analysis was performed. In addition to gradient echo images, conventional T1-weighted images, 2-weighted images with and without fluid attenuation inversion recovery (FLAIR) preparation, and contrast-enhanced T1-weighted images were obtained.

Three observers comprising two neurologists and one neuroradiologist evaluated demyelinating lesions with a long axis ≥3 mm on T2-weighted images with or without FLAIR preparation on a consensus basis. The MRI findings for each lesion were assessed based on QSM and all available MRI images. Based on previous literature,[15] the presence of paramagnetic rims was assessed for each lesion using QSM. Briefly, positivity for paramagnetic rims was considered to be present when hyperintense T2-weighted lesions had a bright surrounding rim in QSM, because paramagnetic substances and tissues are hyperintense in QSM.[21,23] In addition, the lesion location and the presence of contrast enhancement were assessed. For the subject-based analysis, each subject was classified according to the presence or absence of a paramagnetic rim lesion.

For patients who underwent two or more MRI scans, changes in serial findings were evaluated based on the presence of new lesions, contrast enhancement, and paramagnetic rims.

Statistical analysis

Sex, treatment, disease status, frequency of T2-weighted lesions, and paramagnetic rim lesions were compared using Fisher's exact test or the chi-square test. The age, disease duration, and EDSS score in each group were compared using the Wilcoxon rank-sum test. The sensitivity and specificity for the presence of a paramagnetic rim in the differential diagnosis of MS and NMOSD were calculated. The presence of contrast enhancement was assessed according to the presence of a paramagnetic rim. Additional analyses were performed for patients with follow-up examinations, to compare those with and without new lesions, those with and without newly observed paramagnetic rims, and those with and without new contrast-enhanced lesions. All analyses were performed with R statistical software (version 3.5.3, R Foundation, Vienna, Austria; www.R-project.org).

RESULTS

Baseline characteristics

This study included 32 MS patients (7 males and 25 females; age 35.0±10.6 years, mean±standard deviation) and 21 NMOSD

Table 1. Characteristics of the MS and NMOSD patients

	MS	NMOSD	*p*
Number of patients	32	21	-
Sex, male:female	7:25	2:19	0.425
Age, years	35.0±10.6	49.0±14.4	<0.001
Disease duration at first MRI scan, months	33.1 [3.2–66.6]	20.9 [0.8–109.4]	0.993
EDSS score at first MRI scan	1.75 [1.0–2.5]	3.00 [1.0–3.5]	0.024
Patients with follow-up MRI scans	22 (68.8)	12 (57.1)	0.211
Number of MRI scans	71	35	-
Number of MRI scans per patient	2.2±1.1	1.7±1.0	0.071
Treatment received at MRI scans	50/71 (70.4)	20/35 (57.1)	0.254
MRI scans in the acute phase of clinical attacks*	10/71 (14.1)	17/35 (48.6)	<0.01
Per-patient analysis			
T2-weighted lesions	32/32 (100.0)	13/21 (61.9)	0.001
T2-weighted lesions with paramagnetic rims	27/32 (84.4)	1/21 (4.8)	<0.001
T2-weighted lesions with paramagnetic rims in patients with brain lesions	27/32 (84.4)	1/13 (7.7)	<0.001
Contrast-enhanced lesions	11/32 (34.4)	5/21 (23.8)	0.608
Number of T2-weighted lesions per patient	12.2±8.6	5.6±7.9	0.001
Numbers of T2-weighted lesions with paramagnetic rims per patient	6.5±8.9	0.9±4.1	<0.001
Per-lesion analysis			
T2-weighted lesions	388	117	
T2-weighted lesions with paramagnetic rims	211/388 (54.4)	19/117 (16.2)	<0.001

Data are mean±standard deviation, *n* (%), or median [interquartile range] values.
*Attacks in any location of the central nervous system, including the brain, optic nerve, or spinal cord.
EDSS: Expanded Disability Status Scale, MRI: magnetic resonance imaging, MS: multiple sclerosis, NMOSD: neuromyelitis optica spectrum disorder.

patients (2 males and 19 females; age 49.0±14.4 years) (Table 1). The MS group was significantly younger than the NMOSD group (p<0.001). The first MRI session with QSM was performed when the disease duration was a median of 33.1 months [interquartile range (IQR)=3.2–66.6 months] for MS and 20.9 months (IQR=0.8–109.4 months) for NMOSD. Follow-up MRI examinations including QSM were performed in 22 MS and 12 NMOSD patients, at intervals ranging from 1 month to 14 months. Totals of 71 and 35 MRI scans were performed during the study period in MS and NMOSD patients, respectively. The numbers of MRI examinations in each MS and NMOSD patient were 2.2±1.1 and 1.7±1.0, respectively (Table 1).

Fifty (70.4%) of the 71 MRI scans in MS patients were performed when they were receiving disease-modifying therapies (DMTs): interferon (IFN) β-1a (n=29, 40.8%), IFN β-1b (n=9, 12.7%), glatiramer acetate (n=4, 5.7%), teriflunomide (n=7, 9.9%), or dimethyl fumarate (n=1, 1.4%). Twenty (57.1%) of the 35 MRI scans in NMOSD patients were performed under immunosuppressant therapies: oral steroid alone (n=7, 20.0%), azathioprine (n=4, 11.4%), mycophenolate (n=6, 17.1%), or rituximab (n=2, 5.7%). One (2.9%) of the MRI scans was performed while the patient was receiving treatment with hydroxychloroquine for systemic lupus erythematosus.

Ten (14.1%) of the 71 MRI scans in MS patients were performed in the acute phase, within 1 month after clinical attacks: optic neuritis (n=1), myelitis (n=3), brain symptoms (n=5), and myelitis with brain symptom (n=1). Seventeen (48.6%) of the 35 MRI scans in NMOSD patients were performed in the acute phase: optic neuritis (n=8), myelitis (n=6), brain symptoms (n=2), and optic neuritis with brain symptoms (n=1). The interval between the onset of clinical symptoms and MRI scanning being performed was 9.20±6.81 days (range 1–21 days, median 7 days) in the MS patients and 6.71±5.89 days (range 1–21 days, median 6 days) in the NMOSD patients.

Paramagnetic rims in QSM as a diagnostic imaging marker

Brain lesions were found by T2-weighted MRI in all of the MS patients and in 13 (61.9%) of the NMOSD patients. In the QSM images, lesions with paramagnetic rims were found in 27 (84.4%) of the patients with MS (Figs. 1 and 2) and only 1 (4.8%) of the patients with NMOSD (p<0.001) (Fig. 3A) during follow-up. When considering only patients with brain lesions, 84.4% (27/32) of MS patients and 7.7% (1/13) of NMOSD patients had paramagnetic rim lesions. The presence of at least one paramagnetic rim lesion in QSM distinguished MS from NMOSD with a sensitivity of 81% [95% confidence interval (CI)=64–93%] and a specificity of 95% (95% CI=76–100%). Considering only patients with brain lesions yielded similar values for the sensitivity (84%, 95% CI=67–95%) and specificity (92%, 95% CI=64–100%). The presence of new paramagnetic rims during follow-up had an excellent specificity (100%, 95% CI=66–100%) but a low sensitivity (32%, 95% CI=14–55%) for the differential diagnosis.

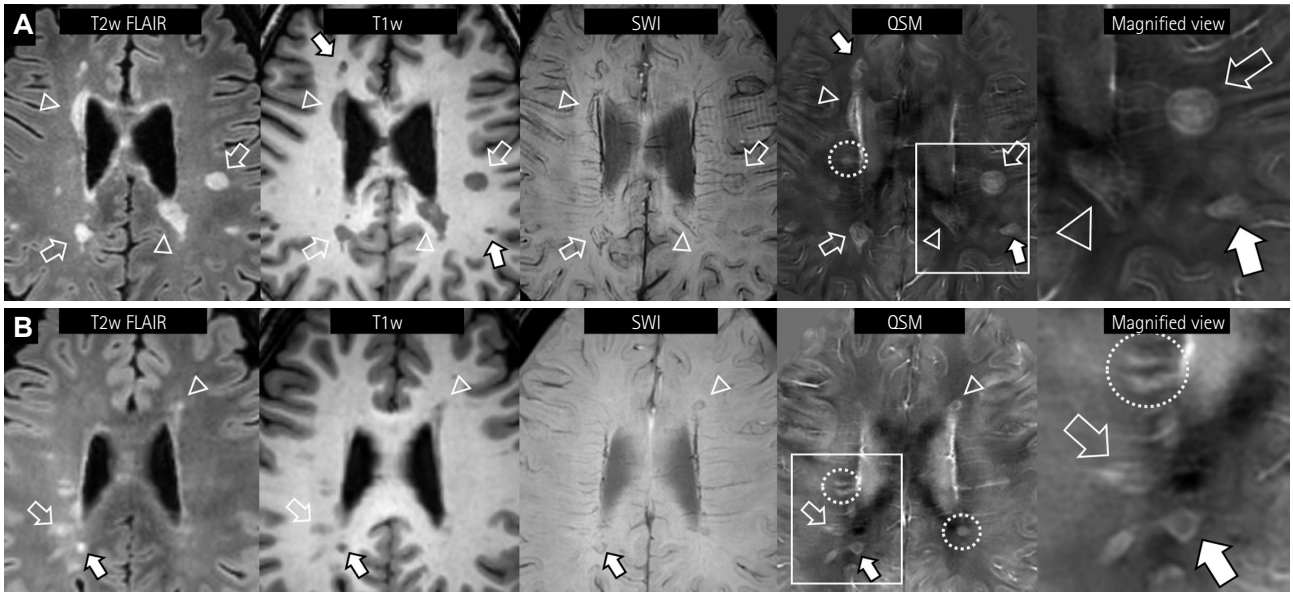

Fig. 1. Representative cases of paramagnetic rim lesions in two MS patients. Subcortical (hollow arrows) and periventricular (hollow arrowheads) lesions of different sizes are observed (A). Subtle and incomplete hypointense rims are observed in SWI. Note the clear and layered paramagnetic rims of MS lesions in QSM images. In another MS patient (B), paramagnetic rims are also observed for small FLAIR lesions in QSM (hollow arrows). In both patients, the T1-weighted black-hole lesion (solid arrows) also shows a QSM rim. Note that while some smaller lesions are paramagnetic, they do not have paramagnetic rims (yellow dotted circles). FLAIR: fluid attenuation inversion recovery, MS: multiple sclerosis, QSM: quantitative susceptibility mapping, SWI: susceptibility-weighted images.

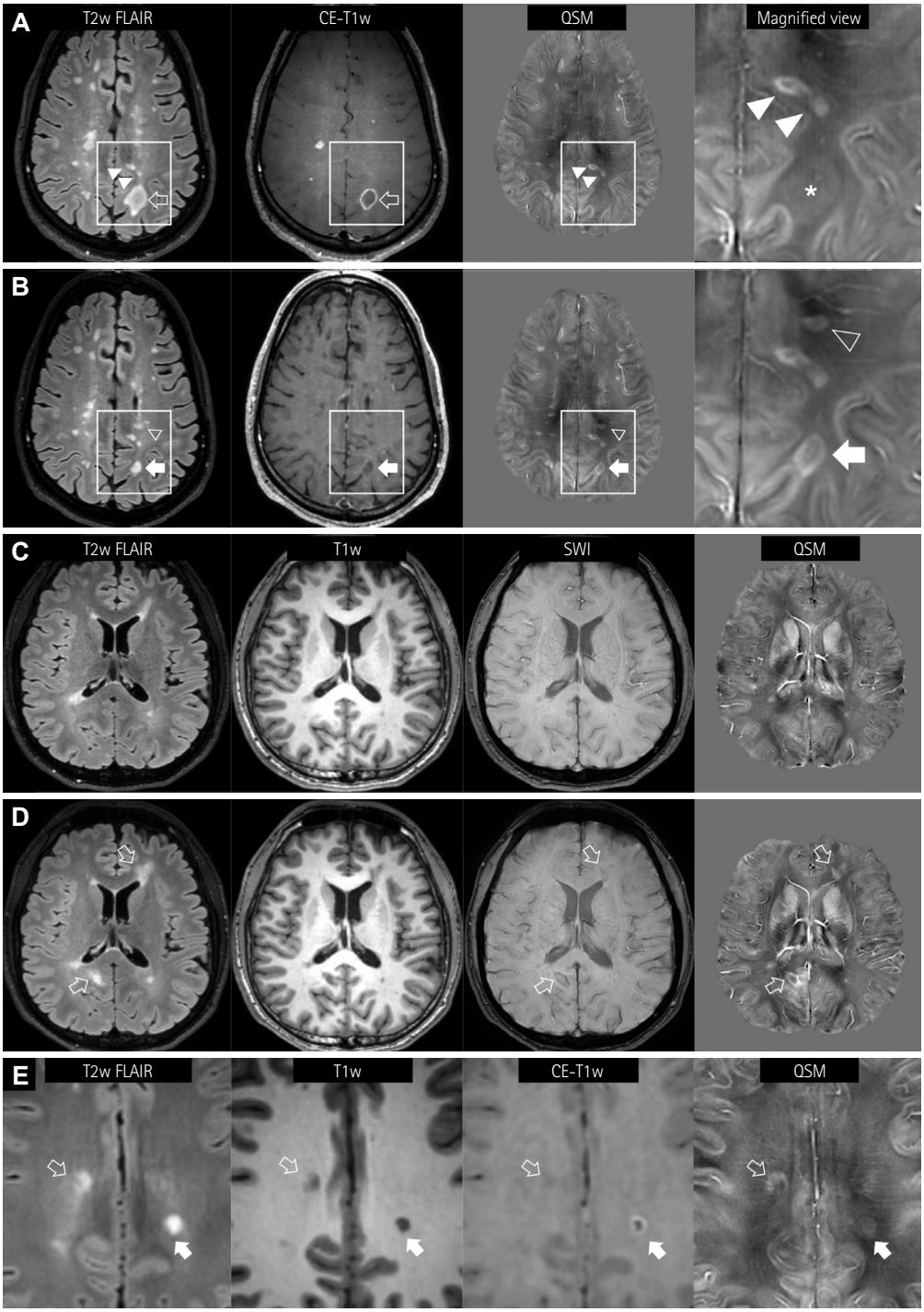

Fig. 2. Longitudinal appearance of QSM rims in MS lesions. A and B: A 44-year-old male patient shows paramagnetic rims (hollow arrow) or nodular enhancements in hyperintense FLAIR lesions (A). A lesion showing a contrast-enhanced rim is slightly paramagnetic (asterisk in the magnified view), suggesting the loss of the diamagnetic myelin tissue. Note the rim or solid paramagnetism in the subcortical FLAIR lesions (solid arrowheads). In follow-up MRI performed 5 months later (B), the size of the FLAIR lesion has decreased (solid arrow) and the enhancement has cleared. The QSM image shows a distinct paramagnetic rim. Additionally, a new periventricular white-matter FLAIR lesion (hollow arrowhead) with a paramagnetic rim is evident. C and D: Another pattern of a new QSM rim lesion in a 23-year-old male MS patient. In the first MRI (C), a small left frontal periventricular lesion is paramagnetic, but it is not accompanied by a paramagnetic rim. At a 9-month follow-up (D), two FLAIR lesions are newly seen (hollow arrows) with paramagnetic rims, with matching dark signals in SWI. E: Another 23-year-old female MS patient shows two subcortical FLAIR lesions with paramagnetic rims in QSM. One lesion shows a complete paramagnetic rim, which is well matched with the enhancement (solid arrow). The other lesion with an irregular and incomplete QSM rim does not exhibit enhancement (hollow arrow). FLAIR: fluid attenuation inversion recovery, MRI: magnetic resonance imaging, MS: multiple sclerosis, QSM: quantitative susceptibility mapping, SWI: susceptibility-weighted images.

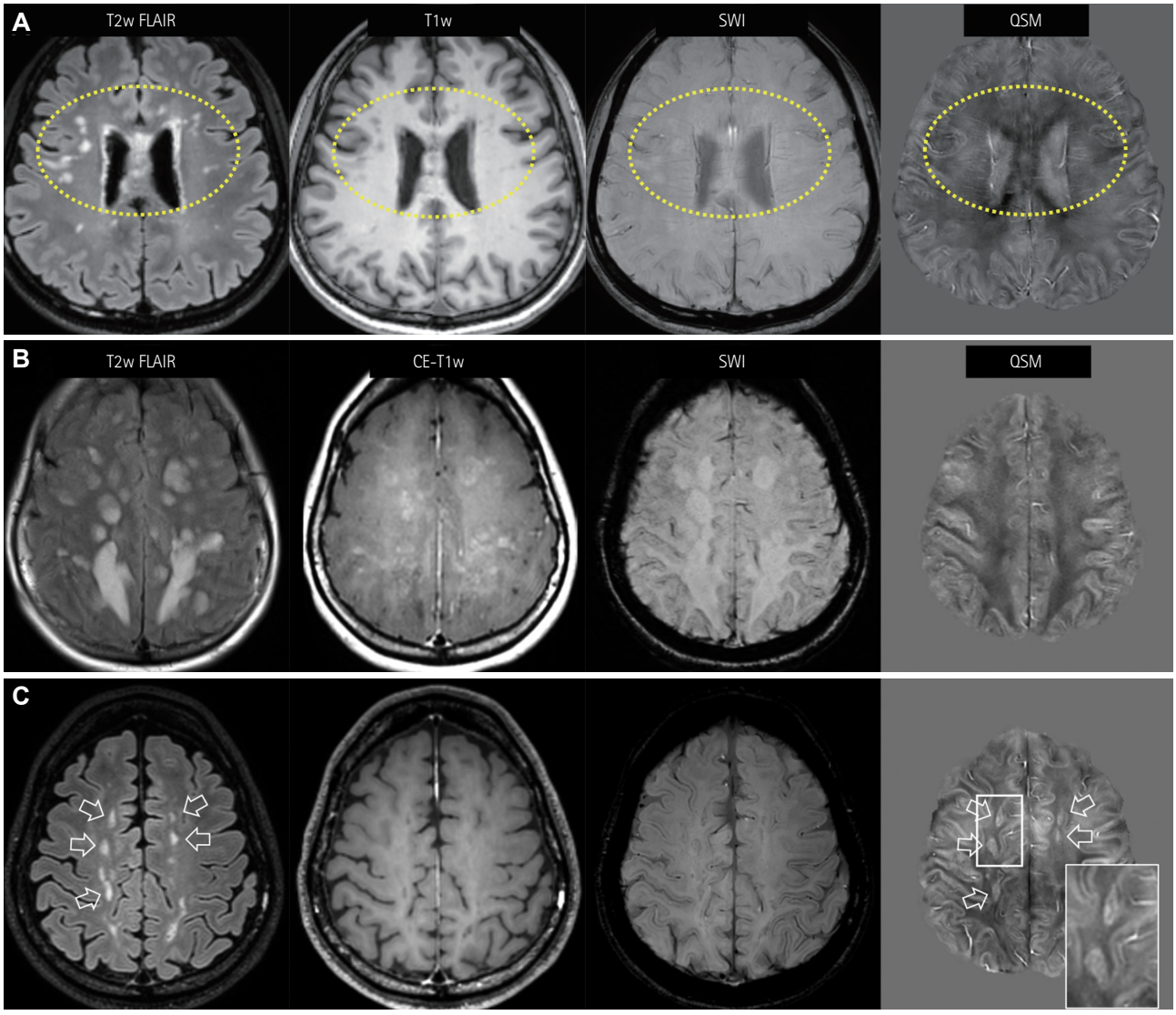

Fig. 3. QSM findings for NMOSD lesions. A: NMOSD lesions without paramagnetic rims in QSM, showing many nodular periventricular and subcortical white-matter lesions in both frontal areas (dotted circles). These lesions do not have dark signals in SWI nor susceptibility changes. B and C: Atypical paramagnetic rims of NMOSD lesions are noted in one patient. The first MRI session (B) shows confluent hyperintense FLAIR lesions. The lesions show patchy or geographic enhancement without susceptibility changes. Follow-up MRI performed 1 year later (C) shows regressed FLAIR lesions (hollow arrows) and enhancement. Some of these lesions show paramagnetic rims in QSM. Note the similarity of the paramagnetic rims (magnified view, box in QSM) with the multiple sclerosis lesions. FLAIR: fluid attenuation inversion recovery, MRI: magnetic resonance imaging, NMOSD: neuromyelitis optica spectrum disorder, QSM: quantitative susceptibility mapping, SWI: susceptibility-weighted images.

Clinical variables such as sex, age, disease duration, EDSS score, clinical status relating to relapse, and whether or not the patients were receiving DMTs did not differ significantly between MS patients with and without paramagnetic rim lesions (Table 2).

Characteristic MRI findings of paramagnetic rim lesions

Location and shape of the paramagnetic rims

The location of the T2-weighted lesions with paramagnetic rims varied, even for characteristic MS lesions in the periventricular or cortical-juxtacortical areas (Fig. 1). In most cases, multiple lesions with paramagnetic rims were observed in diverse locations at the same time. It was particularly interesting that paramagnetic rims were not found in the infratentorial lesions. The shapes of paramagnetic rims surrounding T2-weighted lesions differed with the lesion shape (Figs. 1 and 2). Most of the rims were round or oval, and some were incomplete (Fig. 2E). There were lesions with multiple layers of paramagnetic rims (Fig. 1A). Some lesions with paramagnetic rims also exhibited enhancement (Fig.

2E). Contrast enhancement was present in 6.9% (19/275) of the lesions without paramagnetic rims and in 15% (35/230) of the lesions with paramagnetic rims (p=0.0042).

Appearance of new paramagnetic rims during follow-up

Among 32 patients who underwent follow-up MRI (22 MS and 10 NMOSD patients), new T2-weighted lesions were found in 12 MS and 5 NMOSD patients (Table 3). New paramagnetic rims appeared in 8 (36%) of the 22 MS patients, but in only 1 NMOSD patient (p=0.266). There were 33 new T2-weighted lesions in the 12 MS patients, 19 of whom had paramagnetic rims, 9 of which first showed contrast enhancement; the paramagnetic rims were still present in the next MRI scan but the enhancement had disappeared (Fig. 2A and B). In the remaining 10 lesions, the paramagnetic rims appeared simultaneously with the new nonenhanced T2-weighted lesions

Table 2. Comparison of MS lesions with and without paramagnetic rims

	MS lesions with paramagnetic rims	MS lesions without paramagnetic rims	*p*
Number of patients	27	5	-
Sex, male:female	5:22	2:3	0.632
Age, years	30.0 [24.9–41.6]	40.5 [35.5–54.4]	0.098
Disease duration at first MRI scan, months	29.9 [1.3–63.6]	54.4 [47.3–66.2]	0.161
EDSS score at first MRI	1.5 [1.0–2.2]	2.0 [1.0–2.5]	0.832
Per-patient analysis			
Number of T2-weighted lesions	12 [7–16]	5 [5–12]	0.076
	13.0±9.0	8.0±5.2	0.240
Contrast-enhanced lesions	9/27 (33.3)	2/5 (40.0)	1.000
Per-MRI analysis			
Number of MRI scans	58	13	
Age, years	29.9 [24.8–39.7]	40.5 [27.4–54.4]	0.071
Disease duration, months	33.1 [7.2–67.9]	49.9 [25.9–62.0]	0.624
Disease-modifying therapy	42 (72.4)	8 (61.5)	0.660
MRI scans in the acute phase of clinical attacks*	7 (12.1)	3 (23.1)	0.555

Data are mean±standard deviation, *n* (%), or median [interquartile range] values.
*Attacks in any location of the central nervous system, including the brain, optic nerve, or spinal cord.
EDSS: Expanded Disability Status Scale, MRI: magnetic resonance imaging, MS: multiple sclerosis.

Table 3. Comparison of follow-up MRI scans in MS and NMOSD patients

	MS	NMOSD	*p*
Number of patients	22	10	-
Sex, male:female	5:17	0:10	0.264
Age, years	33.2±9.5	51.8±13.7	<0.001
Disease duration to first MRI scan, months	30.9 [4.3–54.4]	30.2 [0.4–185.2]	0.617
Disease duration to last MRI scan, months	42.3 [13.0–66.9]	37.9 [13.4–197.7]	0.675
Follow-up duration, months	15.8 [10.7–26.4]	14.2 [9.7–16.6]	0.204
EDSS score	1.2 [1.0–2.5]	3.0 [1.5–3.5]	0.029
Per-patient analysis			
New T2-weighted lesions	12/22 (54.5)	5/10 (50.0)	1.000
New lesions with paramagnetic rims	8/22 (36.4)	1/10 (10.0)	0.266
New contrast-enhanced lesions	5/22 (22.7)	3/10 (30.0)	1.000
Number of lesions	12 [6–16]	8 [3–19]	0.554
Numbers of lesions with paramagnetic rims	3.5 [1–8]	0 [0–0]	0.002
Per-lesion analysis			
Number of lesions at last MRI scan	282	105	
New T2-weighted lesions	33 (11.7)	33 (31.4)	<0.001
New paramagnetic rims	19 (6.7)	19 (18.1)	0.002

Data are mean±standard deviation, *n* (%), or median [interquartile range] values.
EDSS: Expanded Disability Status Scale, MRI: magnetic resonance imaging, MS: multiple sclerosis, NMOSD: neuromyelitis optica spectrum disorder.

(Fig. 2C and D). We observed that none of the paramagnetic rims in any of the lesions resolved during follow-up.

An atypical case of NMOSD with paramagnetic rims

One 1 of the 21 NMOSD patients had paramagnetic rims. This 33-year-old patient experienced her first episode of optic neuritis without other symptoms, and showed seropositivity for anti-AQP4 antibodies, antineutrophil cytoplasmic antibodies, and anti-Sjögren's syndrome A antibodies. A diagnosis of NMOSD was made, but she refused all treatment with immunosuppressive agents. Four months later she had a severe relapse with extensive multiple brain lesions, and she became stuporous. Brain MRI revealed numerous lesions, and many of them had characteristics of typical NMOSD lesions based on their locations and shapes as described previously (Fig. 3B).[5,31] The patient fully recovered after consecutive therapies including high-dose intravenous methylprednisolone and plasmapheresis. In the early phase of her severe relapse, we did not observe any paramagnetic rims. However, after 2 months of treatment, the T2-weighted lesions shrank and paramagnetic rims appeared around some of the lesions (Fig. 3C). The imaging characteristics of the paramagnetic rims in this NMOSD patient were similar to those found in our MS patients. Most of the T2-weighted lesions disappeared later in follow-up MRI, but some with paramagnetic rims remained until the last follow-up MRI performed 2 years later. Lesions with paramagnetic rims remained hyperintense on FLAIR images, while those without paramagnetic rims had nearly completely resolved.

DISCUSSION

This study investigated the brain MRI findings of MS and NMOSD patients, focusing on the presence of paramagnetic rims in QSM and their development. These paramagnetic rims occurred more frequently in MS than in NMOSD. The presence of at least one paramagnetic rim around T2-weighted lesions had good diagnostic performance for the differential diagnosis of MS in our study population, especially in terms of the specificity. Similarly, during the follow-up period, paramagnetic rims developed more frequently in MS patients than in NMOSD patients, although only with marginal statistical significance. Our findings suggest that paramagnetic rims can be a useful imaging marker for differentiating MS from NMOSD.

The differences observed in this study may reflect variations on the patterns of lesion evolution or iron metabolism between MS and NMOSD.[32,33] In MS, iron is considered to accumulate mostly at the edges of classic, reactive, slowly expanding, chronically present brain lesions.[7] A speculative explanation involves the distribution of iron. Demyelination and the destruction of oligodendrocytes occur at lesion borders, and iron-containing microglia and macrophages that are mainly located at this edge of chronic reactive lesions undergo microglial dystrophy, leading to the deposition of iron within different compartments of the MS lesions.[7,9]

Our observations using 3-T MRI were consistent with those in previous studies using 7-T MRI. A previous case-control study that examined QSM findings in MS and NMOSD using 7-T MRI[15] categorized lesions into four groups, and the study defined nodular or ring-like "iron-laden lesions" as characteristic MRI lesions of MS compared to NMOSD. These lesions were described as being hypointense in SWI and hyperintense in QSM. Ring-like iron-laden lesions were found in 10.1% of the MS patients but in none of the NMOSD patients.[15] In a follow-up study from the same group, the ring-like iron-laden pattern was found in 8 (4.2%) of 191 MS lesions.[34] Another study using 7-T MRI examined paramagnetic nodular or rim-like phase changes in MS and NMOSD patients.[33] Paramagnetic rim-like lesions were observed in 14% of the lesions in MS patients, but only 2% of the lesions in NMOSD patients. The differences in the QSM findings between MS and NMOSD patients that were found in the present study that utilized 3-T MRI were also effective, and similar to the previous study involving 7-T MRI.[15]

In our study, the proportions of the lesions with paramagnetic rims in the MS and NMOSD patients were 54.4% and 16.2%, respectively. These values are much higher than in previous reports,[34,35] for which we do not have a definitive explanation. However, one possible explanation is that some of the patients in our study had large numbers of T2-weighted lesions, most of which had paramagnetic rims; for example, 2 of our MS patients had 43 and 24 T2-weighted lesions, all of which lesions had paramagnetic rims.

The present review of the serial MRI findings revealed the development of new paramagnetic rim lesions, which has not been intensively studied previously. About one-third of the MS patients who underwent follow-up MRI over approximately 3 years showed new paramagnetic rims. In about half of the new lesions with paramagnetic rims, we first observed contrast enhancement, and then the development of paramagnetic rims while the initial enhancement disappeared. In the other half of the new lesions, paramagnetic rims appeared around new nonenhanced T2-weighted lesions. Although the time interval between the MRI scans might have affected the findings of this study, our results suggest that histopathologic changes occur during the evolution of the lesions in MS. The initial increase in susceptibility in active lesions occurring within weeks in previous studies might be related to the digestion of myelin,[36] while the subsequent increase that occurs over months is more likely to be related to the removal of myelin debris within macrophages[37] and the release of iron.[23,38] The presence

of paramagnetic rims might also indicate chronic active inflammation, which requires close observation.[16,20,21,39] The relatively short study period and low disease activity of our cohort might have limited the clinical validation of newly appearing paramagnetic rims, but further observations will clarify the clinical significance of these findings in MS.

We examined the clinical features of MS patients with and without paramagnetic rims around lesions. Patients with paramagnetic rims were younger and had a marginally shorter disease duration. However, the EDSS score did not differ significantly between these two groups. Considering that demyelinating plaques at different pathologic stages can be simultaneously present in the same MS patient, iron can be deposited around a lesion any time during the course of the disease.

In this study we did not perform a detailed exploration of the contribution of biochemical components of demyelinating lesions to susceptibility. While iron accumulation reportedly occurs predominantly in the periphery of MS lesions, some MS lesions do show layered structures or paramagnetism in the central portion. In addition to iron, myelin has opposite magnetic susceptibility and demyelination contributes to increasing magnetic susceptibility.[40] These factors might explain the heterogeneous appearance of MS lesions (Fig. 2A) as well as the longitudinal changes in their susceptibility.[17,18,35] Unfortunately, current QSM techniques cannot differentiate the contributions of iron deposition and myelin tissue loss to magnetic susceptibility. MRI techniques that can separate the contributions of iron and myelin[41] or which can be selectively specific for each contribution might be helpful.

It was particularly interesting that paramagnetic rims were observed in only one NMOSD patient. The paramagnetic rims in that patient appeared during the recovery phase of multiple extensive brain lesions. Our results are consistent with those of previous studies using 7-T MRI, in which paramagnetic lesions were either absent[15] or present in only 2%[33] of the NMOSD lesions, suggesting that the typical pathomechanism behind the development of brain lesions—including demyelination and iron accumulation—differ between NMOSD and MS. There is a previous report of iron deposition in the deep gray matter of NMOSD patients, although the amount of iron was less than in MS patients.[42] The pathomechanism of paramagnetic rims in NMOSD remains to be clarified, including the contribution of iron to lesion development. Further studies are needed to confirm the histopathologic findings of NMOSD lesions with paramagnetic rims.

The limitations of our study include the relatively small number of patients. The number of NMOSD patients with brain lesions was especially small, and the proportion of patients with paramagnetic rims might not be representative. We used two different MRI devices according to clinical circumstances, which might have introduced unexpected bias into the MRI findings. However, QSM is a quantitative mapping method and it is less affected by MRI parameters and hardware. The use of QSM might have reduced the variability inherent in approaches using conventional MRI. In addition, we did not observe any effect of DMTs on the QSM findings for MS lesions. Lastly, follow-up MRI scans were not performed in all patients, and the follow-up intervals for MRI were not strictly controlled. Future studies should use longer follow-ups with larger populations in order to fully elucidate the clinical significance of paramagnetic rims.

In conclusion, the use of QSM with 3-T MRI allows paramagnetic rims around FLAIR lesions to be used to differentiate MS from NMOSD. Paramagnetic rims occurred in about one-third of MS patients during a 3-year follow-up in this study. About half of the new paramagnetic rim lesions showed contrast enhancement prior to their development. While our findings suggest that paramagnetic rims have diagnostic value in differentiating MS from NMOSD, one atypical NMOSD case was observed with a paramagnetic rim. Further studies with larger study populations and longer follow-ups are needed to clarify the clinical usefulness of the present QSM findings in MS and NMOSD.

Author Contributions

Conceptualization: Jinhee Jang, Woojun Kim. Data curation Jinhee Jang, Yoonho Nam, Kwang-Soo Lee, Woojun Kim. Formal analysis: Jinhee Jang, Woojun Kim. Funding acquisition: Jinhee Jang. Investigation: Jinhee Jang, Yoonho Nam, Woojun Kim. Methodology: Jinhee Jang, Yoonho Nam, Woojun Kim. Project administration: Jinhee Jang, Woojun Kim. Supervision; Kook-Jin Ahn, Bum-soo Kim, Kwang-Soo Lee. Validation: Yoonho Nam, Yangsean Choi, Na-Young Shin, Jae Young An. Visualization: Jinhee Jang, Yangsean Choi, Na-Young Shin. Writing—original draft: Jinhee Jang, Woojun Kim. Writing—review & editing: all authors.

ORCID iDs

Jinhee Jang	https://orcid.org/0000-0002-3386-1208
Yoonho Nam	https://orcid.org/0000-0003-2149-0072
Yangsean Choi	https://orcid.org/0000-0003-1674-7101
Na-Young Shin	https://orcid.org/0000-0003-1157-6366
Jae Young An	https://orcid.org/0000-0002-5131-9164
Kook-Jin Ahn	https://orcid.org/0000-0001-6081-7360
Bum-soo Kim	https://orcid.org/0000-0002-3870-6813
Kwang-Soo Lee	https://orcid.org/0000-0002-6428-5995
Woojun Kim	https://orcid.org/0000-0001-8204-8881

Conflicts of Interest

The authors have no potential conflicts of interest to disclose.

Acknowledgements

We are grateful to Jiwoong Kim, PhD, for contributing to the manuscript preparation. This study was supported by the Basic Science Research Program through the National Research Foundation of Korea funded by the Ministry of Education (NRF-2017R1D1A1B03033829).

REFERENCES

1. Nylander A, Hafler DA. Multiple sclerosis. *J Clin Invest* 2012;122:1180-1188.
2. Kim W, Park MS, Lee SH, Kim SH, Jung IJ, Takahashi T, et al. Characteristic brain magnetic resonance imaging abnormalities in central nervous system aquaporin-4 autoimmunity. *Mult Scler* 2010;16:1229-1236.
3. Kim W, Kim SH, Kim HJ. New insights into neuromyelitis optica. *J Clin Neurol* 2011;7:115-127.
4. Thompson AJ, Banwell BL, Barkhof F, Carroll WM, Coetzee T, Comi G, et al. Diagnosis of multiple sclerosis: 2017 revisions of the McDonald criteria. *Lancet Neurol* 2018;17:162-173.
5. Wingerchuk DM, Banwell B, Bennett JL, Cabre P, Carroll W, Chitnis T, et al. International consensus diagnostic criteria for neuromyelitis optica spectrum disorders. *Neurology* 2015;85:177-189.
6. Al-Radaideh AM, Wharton SJ, Lim SY, Tench CR, Morgan PS, Bowtell RW, et al. Increased iron accumulation occurs in the earliest stages of demyelinating disease: an ultra-high field susceptibility mapping study in clinically isolated syndrome. *Mult Scler* 2013;19:896-903.
7. Bagnato F, Hametner S, Yao B, van Gelderen P, Merkle H, Cantor FK, et al. Tracking iron in multiple sclerosis: a combined imaging and histopathological study at 7 Tesla. *Brain* 2011;134:3602-3615.
8. Hametner S, Wimmer I, Haider L, Pfeifenbring S, Brück W, Lassmann H. Iron and neurodegeneration in the multiple sclerosis brain. *Ann Neurol* 2013;74:848-861.
9. Mehta V, Pei W, Yang G, Li S, Swamy E, Boster A, et al. Iron is a sensitive biomarker for inflammation in multiple sclerosis lesions. *PLoS One* 2013;8:e57573.
10. Wisnieff C, Ramanan S, Olesik J, Gauthier S, Wang Y, Pitt D. Quantitative susceptibility mapping (QSM) of white matter multiple sclerosis lesions: interpreting positive susceptibility and the presence of iron. *Magn Reson Med* 2015;74:564-570.
11. Williams R, Buchheit CL, Berman NE, LeVine SM. Pathogenic implications of iron accumulation in multiple sclerosis. *J Neurochem* 2012;120:7-25.
12. Langkammer C, Schweser F, Krebs N, Deistung A, Goessler W, Scheurer E, et al. Quantitative susceptibility mapping (QSM) as a means to measure brain iron? A post mortem validation study. *Neuroimage* 2012;62:1593-1599.
13. Wang Y, Liu T. Quantitative susceptibility mapping (QSM): decoding MRI data for a tissue magnetic biomarker. *Magn Reson Med* 2015;73:82-101.
14. Liu C, Li W, Tong KA, Yeom KW, Kuzminski S. Susceptibility-weighted imaging and quantitative susceptibility mapping in the brain. *J Magn Reson Imaging* 2015;42:23-41.
15. Chawla S, Kister I, Wuerfel J, Brisset JC, Liu S, Sinnecker T, et al. Iron and non-iron-related characteristics of multiple sclerosis and neuromyelitis optica lesions at 7T MRI. *AJNR Am J Neuroradiol* 2016;37:1223-1230.
16. Zhang Y, Gauthier SA, Gupta A, Tu L, Comunale J, Chiang GC, et al. Magnetic susceptibility from quantitative susceptibility mapping can differentiate new enhancing from nonenhancing multiple sclerosis lesions without gadolinium injection. *AJNR Am J Neuroradiol* 2016;37:1794-1799.
17. Harrison DM, Li X, Liu H, Jones CK, Caffo B, Calabresi PA, et al. Lesion heterogeneity on high-field susceptibility MRI is associated with multiple sclerosis severity. *AJNR Am J Neuroradiol* 2016;37:1447-1453.
18. Chen W, Gauthier SA, Gupta A, Comunale J, Liu T, Wang S, et al. Quantitative susceptibility mapping of multiple sclerosis lesions at various ages. *Radiology* 2014;271:183-192.
19. Gho SM, Liu C, Li W, Jang U, Kim EY, Hwang D, et al. Susceptibility map-weighted imaging (SMWI) for neuroimaging. *Magn Reson Med* 2014;72:337-346.
20. Dal-Bianco A, Grabner G, Kronnerwetter C, Weber M, Höftberger R, Berger T, et al. Slow expansion of multiple sclerosis iron rim lesions: pathology and 7 T magnetic resonance imaging. *Acta Neuropathol* 2017;133:25-42.
21. Absinta M, Sati P, Fechner A, Schindler MK, Nair G, Reich DS. Identification of chronic active multiple sclerosis lesions on 3T MRI. *AJNR Am J Neuroradiol* 2018;39:1233-1238.
22. Absinta M, Sati P, Masuzzo F, Nair G, Sethi V, Kolb H, et al. Association of chronic active multiple sclerosis lesions with disability in vivo. *JAMA Neurol* 2019;76:1474-1483.
23. Zhang S, Nguyen TD, Hurtado Rúa SM, Kaunzner UW, Pandya S, Kovanlikaya I, et al. Quantitative susceptibility mapping of time-dependent susceptibility changes in multiple sclerosis lesions. *AJNR Am J Neuroradiol* 2019;40:987-993.
24. Absinta M, Sati P, Reich DS. Advanced MRI and staging of multiple sclerosis lesions. *Nat Rev Neurol* 2016;12:358-368.
25. Traboulsee A, Simon JH, Stone L, Fisher E, Jones DE, Malhotra A, et al. Revised recommendations of the consortium of MS centers task force for a standardized MRI protocol and clinical guidelines for the diagnosis and follow-up of multiple sclerosis. *AJNR Am J Neuroradiol* 2016;37:394-401.
26. Schofield MA, Zhu Y. Fast phase unwrapping algorithm for interferometric applications. *Opt Lett* 2003;28:1194-1196.
27. Li W, Avram AV, Wu B, Xiao X, Liu C. Integrated laplacian-based phase unwrapping and background phase removal for quantitative susceptibility mapping. *NMR Biomed* 2014;27:219-227.
28. Smith SM. Fast robust automated brain extraction. *Hum Brain Mapp* 2002;17:143-155.
29. Li W, Wang N, Yu F, Han H, Cao W, Romero R, et al. A method for estimating and removing streaking artifacts in quantitative susceptibility mapping. *Neuroimage* 2015;108:111-122.
30. Haacke EM, Liu S, Buch S, Zheng W, Wu D, Ye Y. Quantitative susceptibility mapping: current status and future directions. *Magn Reson Imaging* 2015;33:1-25.
31. Kim HJ, Paul F, Lana-Peixoto MA, Tenembaum S, Asgari N, Palace J, et al. MRI characteristics of neuromyelitis optica spectrum disorder: an international update. *Neurology* 2015;84:1165-1173.
32. Brück W, Popescu B, Lucchinetti CF, Markovic-Plese S, Gold R, Thal DR, et al. Neuromyelitis optica lesions may inform multiple sclerosis heterogeneity debate. *Ann Neurol* 2012;72:385-394.
33. Sinnecker T, Schumacher S, Mueller K, Pache F, Dusek P, Harms L, et al. MRI phase changes in multiple sclerosis vs neuromyelitis optica lesions at 7T. *Neurol Neuroimmunol Neuroinflamm* 2016;3:e259.
34. Chawla S, Kister I, Sinnecker T, Wuerfel J, Brisset JC, Paul F, et al. Longitudinal study of multiple sclerosis lesions using ultra-high field (7T) multiparametric MR imaging. *PLoS One* 2018;13:e0202918.
35. Bozin I, Ge Y, Kuchling J, Dusek P, Chawla S, Harms L, et al. Magnetic resonance phase alterations in multiple sclerosis patients with short and long disease duration. *PLoS One* 2015;10:e0128386.
36. Deh K, Ponath GD, Molvi Z, Parel GT, Gillen KM, Zhang S, et al. Magnetic susceptibility increases as diamagnetic molecules breakdown: myelin digestion during multiple sclerosis lesion formation contributes to increase on QSM. *J Magn Reson Imaging* 2018;48:1281-1287.
37. Kuhlmann T, Ludwin S, Prat A, Antel J, Brück W, Lassmann H. An updated histological classification system for multiple sclerosis lesions. *Acta Neuropathol* 2017;133:13-24.
38. Zhang Y, Gauthier SA, Gupta A, Chen W, Comunale J, Chiang GC, et al. Quantitative susceptibility mapping and R2* measured changes during white matter lesion development in multiple sclerosis: myelin breakdown, myelin debris degradation and removal, and iron accumulation. *AJNR Am J Neuroradiol* 2016;37:1629-1635.
39. Lucchinetti C, Brück W, Parisi J, Scheithauer B, Rodriguez M, Lassmann H. Heterogeneity of multiple sclerosis lesions: implications for the pathogenesis of demyelination. *Ann Neurol* 2000;47:707-717.

40. Wiggermann V, Hametner S, Hernández-Torres E, Kames C, Endmayr V, Kasprian G, et al. Susceptibility-sensitive MRI of multiple sclerosis lesions and the impact of normal-appearing white matter changes. *NMR Biomed* 2017;30.e3727.
41. Lee J, Nam Y, Choi JY, Shin H, Hwang T, Lee J. *Separating positive and negative susceptibility sources in QSM*. Proceedings of the ISMRM 25th Annual Meeting & Exhibition; 2017 Apr 22-27 Honolulu, HI. Concord, CA: International Society for Magnetic Resonance in Medicine, 2017.
42. Chen JJ, Carletti F, Young V, Mckean D, Quaghebeur G. MRI differential diagnosis of suspected multiple sclerosis. *Clin Radiol* 2016;71:815-827.